1156–1163 *Nucleic Acids Research, 2003, Vol. 31, No. 4*
DOI: 10.1093/nar/gkg211

Structural transition from antiparallel to parallel G-quadruplex of d($G_4T_4G_4$) induced by Ca^{2+}

Daisuke Miyoshi[1], Akihiro Nakao[1] and Naoki Sugimoto[1,2,*]

[1]Department of Chemistry, Faculty of Science and Engineering and [2]High Technology Research Center, Konan University, 8-9-1 Okamoto, Higashinada-ku, Kobe 658-8501, Japan

Received November 14, 2002; Revised and Accepted December 13, 2002

ABSTRACT

Guanine quadruplex (G-quadruplex) structures are formed by guanine-rich oligonucleotides. Because of their *in vivo* and *in vitro* importance, numerous studies have been demonstrated that the structure and stability of the G-quadruplex are dependent on the sequence of oligonucleotide and environmental conditions such as existing cations. Previously, we quantitatively investigated the divalent cation effects on the antiparallel G-quadruplex of d($G_4T_4G_4$), and found that Ca^{2+} induces a structural transition from the antiparallel to parallel G-quadruplex, and finally G-wire formation. In the present study, we report in detail the kinetic and thermodynamic analyses of the structural transition induced by Ca^{2+} using stopped-flow apparatus, circular dichroism, size-exclusion chromatography (SEC) and atomic force microscopy. The quantitative parameters showed that at least two Ca^{2+} ions were required for the transition. The kinetic parameters also indicated that d($G_4T_4G_4$) underwent the transition through multiple steps involving the Ca^{2+} binding, isomerization and oligomerization of d($G_4T_4G_4$). The parallel-stranded G-wire structure of d($G_4T_4G_4$), which is a well controlled alignment of numerous DNA strands with G-quartets, as the final product induced by Ca^{2+}, was observed using SEC and atomic force microscopy. These results provide insight into the mechanism of the structural transition and G-wire formation and are useful for constructing a nanomaterial regulated by Ca^{2+}.

INTRODUCTION

Guanine-rich oligonucleotides fold into guanine quadruplex (G-quadruplex) structures in the presence of certain cations (1–3). While direct evidence of G-quadruplex formation and function *in vivo* is still lacking, there is growing interest in the possible roles of the G-quadruplex structure as lead molecules in drug design, as a general structural motif potentially adopted by telomerase, as the structure in immunoglobin switch regions, as centromere DNA and in other biological systems (4–8). On the other hand, functional molecules such as a thrombin-binding aptamer, an inhibitor of HIV integrase, and a catalytic porphyrin metalation DNA form a G-quadruplex structure *in vitro* (9–12). In addition, the polymorphic nature of the G-quadruplexes is promising for use as nanotechnology materials. Regulating the structural polymorphism of the G-quadruplex can present a novel methodology for controlling biological phenomena, functional molecules, and nanomaterials related to the G-quadruplex.

A higher-order and parallel-stranded G-quadruplex, the so-called G-wire, is an especially useful structure as a nanomaterial because the G-wire has a well controlled and regulated alignment of numerous DNA strands with G-quartets. Previously, we showed that only 1 mM divalent cations destabilize the antiparallel G-quadruplex structure of d($G_4T_4G_4$) and higher concentrations of Ca^{2+} induce a higher-ordered G-quadruplex structure like a G-wire (13). G-wire structures have been observed by other combinations of DNA oligonucleotides and divalent cations. For example, Chen reported a supramolecular self-assembly of d[$(TGG)_4$] induced by Mg^{2+} (14), and an intermolecular G-quadruplex formation of d[$(G_4T_2)_3G_4$] induced by Sr^{2+} (15). Venczel and Sen showed that a parallel G-quadruplex structure of d($TGTG_3TGTGTGTG_3$) in the presence of Mg^{2+} and Ba^{2+} (16). Importantly, Neidle and co-workers reported a model for higher-order telomeric DNA structure at the end of a human chromosome based on the parallel-stranded crystal structure of d[$TAG_3T_2AG_3T$] and d[$AG_3(T_2AG_3)_3$] (17). They revealed that the parallel strands are linked with the trinucleotide loops positioned on the outside of the G-quartets in a propeller-like arrangement, and therefore the folded human G-quadruplex can form a cylindrical quasi-superhelix, like a G-wire, with the stacking interactions between G-quartets (17). However, a mechanism for the structural transition from the antiparallel to parallel G-quadruplex and G-wire formation is not yet clear because only a few quantitative thermodynamic and kinetic parameters of the structural transition and formation have been reported.

In the present study, we report the detailed thermodynamic and kinetic analyses for the antiparallel to parallel structural transition of the G-quadruplex and the G-wire formation of d($G_4T_4G_4$) induced by Ca^{2+}. The parallel-stranded G-wire of d($G_4T_4G_4$) as a final product induced by Ca^{2+} was indicated using size-exclusion chromatography (SEC) and using atomic force microscopy. Although the number of cation bindings for

*To whom correspondence should be addressed at Faculty of Science and Engineering, Konan University, 8-9-1 Okamoto, Higashinada-ku, Kobe 658-8501, Japan. Tel: +81 78 435 2497; Fax: +81 78 435 2539; Email: sugimoto@konan-u.ac.jp

the G-quadruplex is one of the important areas to investigate the G-quadruplex structure, the number of divalent cations such as Mg^{2+}, Ba^{2+} and Sr^{2+} required for the structural transition and G-wire formation was not reported. The equilibrium and kinetic parameters obtained here showed that at least two Ca^{2+} ions were required in the transition. The kinetic parameters also indicated that $d(G_4T_4G_4)$ underwent the transition through multiple steps involving the Ca^{2+} binding, isomerization and oligomerization of $d(G_4T_4G_4)$. The multi-step mechanism is also supported by previous reports of parallel G-quadruplex formations from single strands. Therefore, the mechanism reported here suggests a general mechanism for the parallel G-quadruplex and G-wire formation.

MATERIALS AND METHODS

Material preparations

Oligonucleotides were synthesized on solid supports using standard β-cyanoethyl phosphoramidite methods as described previously (18,19). The synthesized DNA oligonucleotides containing the 5′-end dimethoxytrityl (DMT) groups were removed from the solid support, and base blocking groups were removed by treatment with concentrated 25% ammonia at 55°C for 8 h. After drying in a vacuum, the oligonucleotides were passed through a Poly-Pak cartridge (Glen Research Co., Ltd) with 2% trifluoroacetic acid to remove the 5′-end DMT groups. After deblocking operations, the oligonucleotides were desalted through a C-18 Sep-Pak cartridge column (Waters). The oligonucleotides were purified by reverse-phase high performance liquid chromatography (HPLC) on a TSK-gel Oligo DNA RP column (Tosoh) with a linear gradient of 0–50% MeOH/H_2O containing triethylammonium acetate (pH 7.0). The final purities of the oligonucleotides were confirmed to be >98% by HPLC. The purified oligonucleotides were desalted again with a C-18 Sep-Pak cartridge before use. The single-strand concentrations of the oligonucleotides were determined by measuring the absorbance at 260 nm at high temperature. Single-strand extinction coefficients were calculated from the mononucleotide and dinucleotide data using a nearest-neighbor approximation (20).

Circular dichroism spectra

All the circular dichroism (CD) titration experiments utilizing a JASCO J-820 spectropolarimeter were measured for the 25 μM total strand concentration of oligonucleotides in a 0.1 cm path length cuvette with a buffer containing 50 mM MES (pH 6.1), 100 mM NaCl and the appropriate concentration of $CaCl_2$ at 5°C as described previously (13). Before CD spectroscopy, the DNA sample was heated to 90°C, gently cooled at a rate of 3°C min^{-1}, and incubated at 5°C for several hours.

Size-exclusion chromatography measurements

SEC was performed using a HPLC system equipped with a TSK-gel 2000 (Tosoh) at 25°C. The flow rate was 1.0 ml min^{-1}, and the elution of DNA was monitored by measuring the absorbance at 260 nm with a buffer containing (a) 50 mM MES, (b) 100 mM NaCl and 50 mM MES or (c) 50 mM $CaCl_2$, 100 mM NaCl and 50 mM MES. These buffers were adjusted with LiOH to pH 6.1. Before measurement, the DNA sample was thermally treated as described above and incubated at 25°C for several hours.

Kinetic experiments

The structural transition from the antiparallel to the parallel G-quadruplex of $d(G_4T_4G_4)$ was induced by the addition of $CaCl_2$, which was performed with a stopped-flow apparatus (UNISOKU Inc., Japan) installed in the cell compartment of the J-820. The concentration of $d(G_4T_4G_4)$ before and after mixing was 50 and 25 μM, respectively. The $CaCl_2$ solution contains the same buffer [100 mM NaCl and 50 mM MES (pH 6.1), and the appropriate concentration of $CaCl_2$]. The two solutions were mixed at a ratio of 1:1. Before measurement, the DNA sample was thermally treated as described above and incubated at a measuring temperature for several hours.

Atomic force microscope measurements

The atomic force microscope (AFM) measurements were carried out after a 3-h incubation at 45°C of 25 μM $d(G_4T_4G_4)$ in a buffer containing 100 mM NaCl, 50 mM MES (pH 6.1) with or without 100 mM $CaCl_2$. After incubation, a 1 μl sample was deposited onto freshly cleaved mica three times, washed with 500 μl deionized water three times, dried with a stream of N_2 gas and then the AFM images were obtained in the tapping mode using a Nanoscope III (Digital Instruments Inc., USA).

RESULTS AND DISCUSSION

Ca^{2+} induces the structural transition from antiparallel to parallel G-quadruplex

Figure 1A shows the CD spectra of 25 μM $d(G_4T_4G_4)$, $d(G_3T_3G_3)$ and $d[(G_4T_4)_3G_4]$ in a buffer containing 100 mM NaCl, 50 mM MES (pH 6.1) with or without 100 mM $CaCl_2$ at 5°C. The CD spectra indicate that Ca^{2+} induces the structural transition of the G-quadruplex of all the oligonucleotides from antiparallel to parallel (13). These results demonstrate that the structural transitions of both intermolecular and intramolecular G-quadruplexes were induced by Ca^{2+}, and suggest qualitatively that length of guanine stretch and thymine loop may not have an important role in the transition. The CD intensity at 260 nm is useful for detecting the structural transition between the antiparallel and the parallel G-quadruplexes because the typical CD spectra of the parallel and the antiparallel G-quadruplexes show large positive and large negative peaks near 260 nm, respectively (21,22). Figure 1B shows the CD intensity change of 25 μM $d(G_4T_4G_4)$ at 260 nm versus Ca^{2+} concentration and the best fit results for the data, with the assumptions that the number of Ca^{2+} ions bound is one or variable. The number of Ca^{2+} bound is calculated to be 2.11 ± 0.14 from the latter assumption. Although elucidation of a number of cation bindings for G-quadruplex is generally difficult, the results of the curve fitting indicate that at least two Ca^{2+} ions bind to $d(G_4T_4G_4)$ during the structural transition. The binding constant of Ca^{2+} for $d(G_4T_4G_4)$ was estimated to be 8.41×10^3 M^{-2} or 7.03×10^5 M^{-3} with the assumption that the number of Ca^{2+} bound is two or three, respectively. The coordination number of Ca^{2+} with ligands is six or eight. If Ca^{2+} coordinates to the G-quartets with the

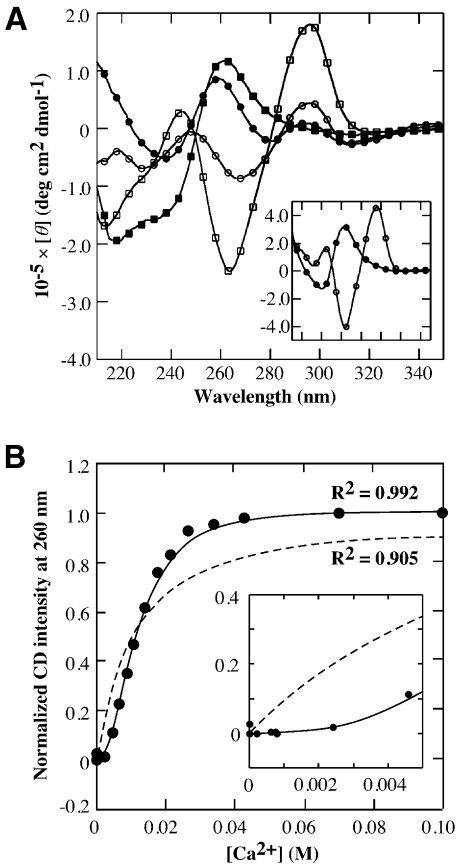

Figure 1. Equilibrium analysis of the transition from the antiparallel to the parallel G-quadruplex. (**A**) CD spectra of 25 μM d($G_4T_4G_4$) (squares), d($G_3T_3G_3$) (circles) and d[(G_4T_4)$_3$$G_4$] (circles in the inset) in a buffer containing 100 mM NaCl, 50 mM MES (pH 6.1) with (filled symbols) or without 100 mM $CaCl_2$ (open symbols) at 5°C. (**B**) Plot of normalized CD intensity d($G_4T_4G_4$) at 260 nm versus Ca^{2+} concentration at 5°C. Dotted and stick lines indicate best-fit results for the data with the following equations: (normalized CD intensity at 260 nm) = $K_a[Ca^{2+}]/(1 + K_a[Ca^{2+}])$ and (normalized CD intensity at 260 nm) = $K_a[Ca^{2+}]^n/(1 + K_a[Ca^{2+}]^n)$, respectively. The best fitted value for n is calculated to be 2.11.

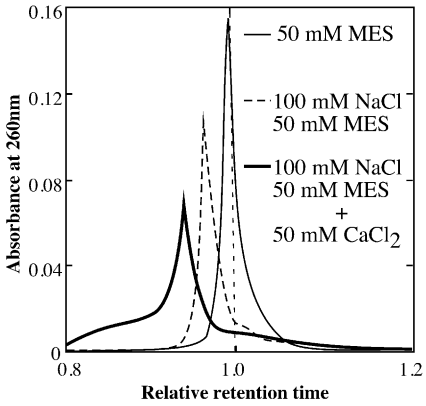

Figure 2. SEC profiles for d($G_4T_4G_4$) in buffers containing 50 mM MES (thin line), 100 mM NaCl and 50 mM MES (dotted line), and 50 mM $CaCl_2$, 100 mM NaCl and 50 mM MES (thick line) at 25°C. These buffers were adjusted with LiOH to pH 6.1. The relative retention times in the buffers were calculated from the observed retention times of d($G_4T_4G_4$) against those for a 12mer DNA marker, d($T_3C_3T_2CT_2$), which forms neither intramolecular nor intermolecular structures under these conditions. In buffer (a), the observed retention times of the marker and d($G_4T_4G_4$) were 7.71 and 7.62 min, respectively. In buffer (b), they were 8.71 and 8.32 min, respectively. In buffer (c), they were 9.89 and 9.29 min, respectively.

octahedral configuration, two Ca^{2+} ions occupy four G-quartets because one G-quartet has four oxygens as ligands. This consideration supports the fact that two Ca^{2+} ions are required for the structural transition. Although it may be possible that the number of Ca^{2+} bound for not only G-quartets but also loop region is three, we can conclude that at least two Ca^{2+} ions are required to the transition.

The formation of the parallel G-quadruplex induced by Ca^{2+} was also confirmed by the SEC profiles of d($G_4T_4G_4$) in buffers containing (a) 50 mM MES (pH 6.1), (b) 100 mM NaCl and 50 mM MES (pH 6.1) and (c) 50 mM $CaCl_2$, 100 mM NaCl and 50 mM MES (pH 6.1) (Fig. 2). To eliminate the effect of the constituents of the buffers on the retention time, the retention times of d($G_4T_4G_4$) in the buffers were evaluated relative to those for a single-stranded 12mer DNA, d($T_3C_3T_3CT_2$), used as a reference. This reference DNA [molecular weight (Mw): 3578.2] does not form a secondary structure even in the presence of a cation. Therefore, d($T_3C_3T_3CT_2$) is useful to elucidate an apparent molecular mass of d($G_4T_4G_4$) (Mw: 3856.4) in the various conditions. In buffer (a), the observed retention times of the marker and d($G_4T_4G_4$) were 7.71 and 7.62 min, respectively. Therefore, the relative retention time of d($G_4T_4G_4$) was 0.989 showing that the apparent molecular mass of d($G_4T_4G_4$) was slightly larger than the reference, and that d($G_4T_4G_4$) exists as a single strand in the absence of Na^+ and Ca^{2+}. In buffer (b), the observed retention times of the marker and d($G_4T_4G_4$) were 8.71 and 8.32 min, respectively. The relative retention time in buffer (b) was calculated to be 0.956. Previously, it was reported that d($G_4T_4G_4$) folds into double-stranded antiparallel G-quadruplex in the presence of Na^+ (23). Therefore, the relative retention time of d($G_4T_4G_4$) in the buffer (b) indicates the antiparallel G-quadruplex formation of d($G_4T_4G_4$) in the presence of Na^+. In buffer (c), the observed retention times of the marker and d($G_4T_4G_4$) were 9.89 and 9.29 min, respectively. The relative retention time in buffer (c) was calculated to be 0.939. These results give apparent molecular masses for d($G_4T_4G_4$) in these buffers as follows: (c) > (b) > (a). This agrees with the CD spectrometry results showing that Ca^{2+} induces a structural transition of the DNA, as shown in Figure 1A.

Kinetic analysis of the structural transition

To investigate the mechanism of the structural transition of d($G_4T_4G_4$) from the antiparallel to the parallel G-quadruplex induced by Ca^{2+}, the kinetics of the structural transition was traced by monitoring the CD intensity at 260 nm and 45°C for varying concentrations of Ca^{2+} (Fig. 3A). Since the melting temperature of d($G_4T_4G_4$) in the presence of 100 mM Na^+ is much higher than 45°C (13), the initial structure of the kinetic curve is the antiparallel G-quadruplex under this condition. The kinetic traces were fitted to a single exponential function to obtain the observed rate constant, k_{obs}. Previous studies showed that monovalent cation binding to the G-quadruplex was very fast (relaxation time was in the order of milliseconds) (24,25). Furthermore, folding kinetics of the *Tetrahymena*

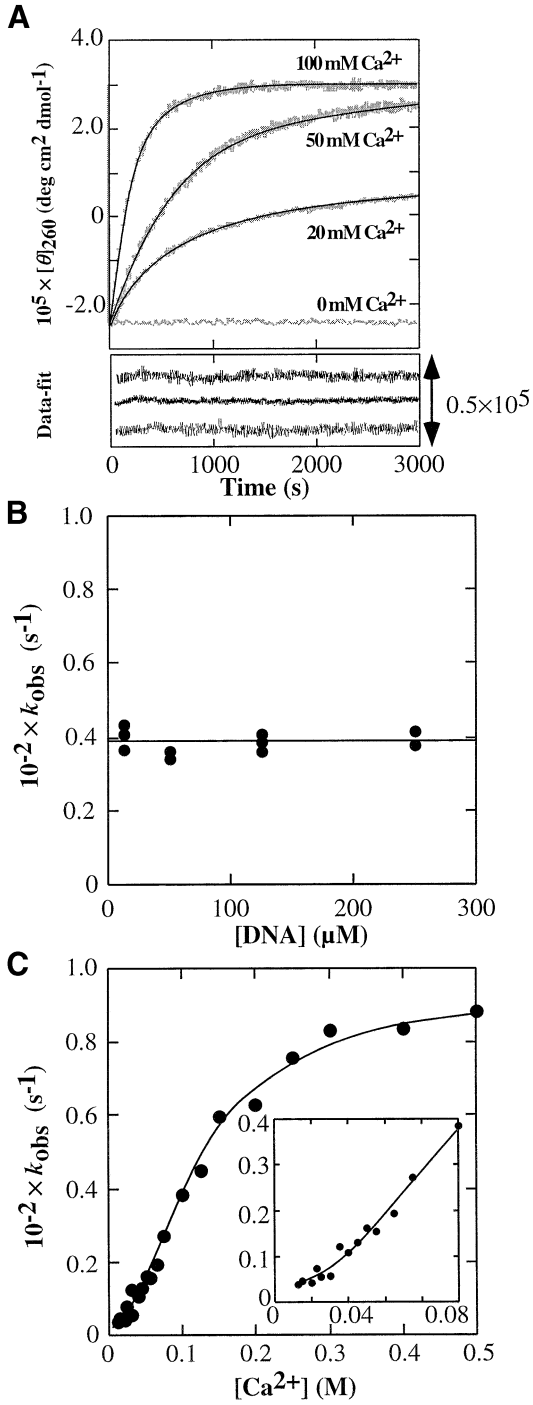

Figure 3. Kinetic properties of the transition of $d(G_4T_4G_4)$ from the antiparallel to the parallel G-quadruplex. (**A**) Kinetic traces of the transition of 25 μM $d(G_4T_4G_4)$ traced with CD intensity at 260 nm. Data were collected immediately after 1:1 mixing of 50 μM $d(G_4T_4G_4)$ and various concentrations of $CaCl_2$. All measurements were performed in a buffer containing 100 mM NaCl and 50 mM MES (pH 6.1) at 45°C. The traces were fitted to a single exponential curve. (**B**) Plot of k_{obs} at 400 mM Ca^{2+} at 40°C versus various concentrations of $d(G_4T_4G_4)$ in a buffer containing 100 mM NaCl and 50 mM MES (pH 6.1). (**C**) Plot of k_{obs} of 25 μM $d(G_4T_4G_4)$ versus concentration of Ca^{2+} at 45°C in a buffer containing 100 mM NaCl and 50 mM MES (pH 6.1). The solid line indicates the best-fit result for the data using equation **2**.

ribozyme induced by Mg^{2+} showed that a stable tertiary intermediate structure is formed with a rate constant of >2 s^{-1} (26,27). This indicates that the divalent cation binding to nucleotides is very fast process. Therefore, it is possible to consider that the kinetic traces obtained here correspond to the antiparallel to parallel structural transition, but not to Ca^{2+} binding for $d(G_4T_4G_4)$. Values for k_{obs} calculated from the kinetic traces induced by 400 mM Ca^{2+} at 40°C were plotted versus the $d(G_4T_4G_4)$ concentration, as shown in Figure 3B. k_{obs} is constant (k_{obs} = 0.394 × 10^{-2} s^{-1}) at various concentrations of $d(G_4T_4G_4)$, indicating that the oligomerization of $d(G_4T_4G_4)$ is not the rate determining step. Investigation of the effect of the Ca^{2+} concentration on k_{obs} showed that maximal k_{obs} is reached at a concentration of 300 mM Ca^{2+}, and k_{obs} decreases with low Ca^{2+} concentrations, as shown in Figure 3C. If the mechanism of the structural transition included only one step when $[Ca^{2+}] >> [d(G_4T_4G_4)]$, the observed rate constant would linearly increase with the $[Ca^{2+}]$, but this is not the case. The simplest mechanism consistent with the results in Figure 3C is a sequential two-step mechanism (28,29), where the process of the structural transition occurs after the Ca^{2+} binding step for the antiparallel $d(G_4T_4G_4)$. From this dependence of k_{obs} on $[Ca^{2+}]$, the rate constants of the structural transition step and binding constant of Ca^{2+} for $d(G_4T_4G_4)$ can be obtained from the following model.

$$\text{Antiparallel} + 2Ca^{2+} \underset{k_{-1}}{\overset{k_{+1}}{\rightleftarrows}} \text{Antiparallel: } 2Ca^{2+} \underset{k_{-2}}{\overset{k_{+2}}{\rightleftarrows}} \text{Parallel: } 2Ca^{2+} \qquad \mathbf{1}$$

where Antiparallel and Parallel indicate the antiparallel and parallel G-quadruplexes of $d(G_4T_4G_4)$, respectively. Since the first step in the mechanism should be very fast as described above and $[Ca^{2+}] >> [\text{Antiparallel}]$, the observed rate constant for this mechanism is the following equation:

$$k_{obs} = \{k_{+2}[Ca^{2+}]_0^2/([Ca^{2+}]_0^2 + 1/K_1)\} + k_{-2} \qquad \mathbf{2}$$

where $[Ca^{2+}]_0$ is the initial concentration of Ca^{2+} and $K_1 = k_{+1}/k_{-1}$. The non-linear least-squares fit of the data to equation **2** is shown in Figure 3C. When the number of bound Ca^{2+} is one, the non-linear least-squares fit of the data to the sequential two-steps model could not give good agreement between the theoretical line and data especially at the lower concentrations of Ca^{2+}. Thus, not only the fitted curve for the equilibrium in Figure 1B but also the curve for the kinetic data in Figure 3C lead to the conclusion that at least two Ca^{2+} ions bind to $d(G_4T_4G_4)$ during the structural transition. The kinetic parameters, K_1, k_{+2} and k_{-2}, are calculated to be 60.4 ± 4.6 M^{-2}, (9.10 ± 0.17) × 10^{-3} s^{-1}, and 3.15 ± 0.86 × 10^{-4} s^{-1}, respectively, with the assumption that the number of Ca^{2+} bound is two (Table 1).

We also investigated the kinetic profile of the transition at various temperatures. The values of k_{+2} at 37, 40, 42.5, 45, 47.5 and 50°C were 1.96 × 10^{-3} s^{-1}, 3.80 × 10^{-3} s^{-1}, 6.73 × 10^{-3} s^{-1}, 9.10 × 10^{-3} s^{-1}, 12.1 × 10^{-3} s^{-1} and 18.0 × 10^{-3} s^{-1},

Table 1. Kinetic and thermodynamic parameters of the structural transition

	K_1 (M^{-2})	$10^3 \times k_{+2}$ (s^{-1})	$10^4 \times k_{-2}$ (s^{-1})	K_2	$10^{-3} \times K_{all}$ (M^{-2})[a]
Kinetic[b]	60.4 ± 4.6	9.10 ± 0.17	3.15 ± 0.86	28.9 ± 11.5	1.75 ± 0.88
Equilibrium[c]	–	–	–	–	8.41 ± 0.50[d]

[a]All of the structural transition estimated from kinetic data was calculated from K_1 and K_2 (= k_{+2}/k_{-2}).
[b]All measurements were performed at 45°C.
[c]All measurements were performed at 5°C.
[d]The binding constant was calculated with the assumption that the number of Ca^{2+} bound is two.

respectively. From the kinetic profile, the activation energy, E_a, of k_{+2} was calculated to be 33.0 ± 2.2 kcal mol^{-1} using the Arrhenius equation (Fig. 4). The activation parameters, $\Delta H^{\ddagger}$ and $\Delta S^{\ddagger}$, were calculated to be 32.4 kcal mol^{-1} and 34.2 cal mol^{-1} K^{-1}, respectively. This activation enthalpy is larger than that for the folding of the 160-nt P4-P6 domain of the *Tetrahymena* group I intron RNA (18–24 kcal mol^{-1}) (30,31), and is similar to that of the Hairpin ribozyme (29 kcal mol^{-1}) (32). Even though larger $\Delta H^{\ddagger}$ values for large RNA folding processes are reported (33,34), the DNA used here comprises only 12 nt, therefore the activation enthalpy of the structural transition indicates that an unusually high activation barrier exists between the antiparallel and the parallel G-quadruplex structures of $d(G_4T_4G_4)$. One possibility is that the large positive activation enthalpy may be interpreted to be due to an unfolding process required for the isomerization from the *anti* to *syn* glycosyl torsion angle of the guanine bases as shown in protein folding and unfolding, in which proline isomerization that is believed to produce slow reactions and intermediate states (35). The positive value of the activation entropy also implies that the transition state is less ordered than the $d(G_4T_4G_4):Ca^{2+}$ intermediate (26). One consideration for such disorder is partial unfolding of some part of $d(G_4T_4G_4)$. An alternative consideration is that the base pairs between the guanine bases may be partly broken in the transition state. In either case, the positive activation entropy also suggests that the process consists of at least two steps including the unfolding step of $d(G_4T_4G_4)$ is required for the isomerization of the guanine bases.

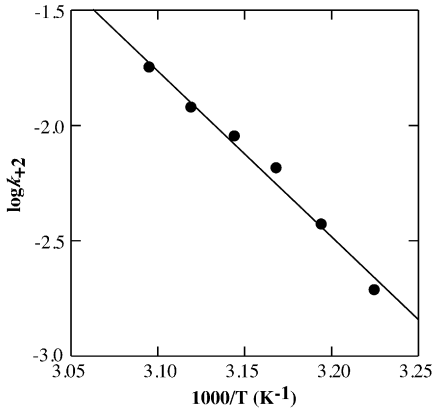

Figure 4. Arrhenius plot of log k_{+2} versus $1/T$. The solid line is obtained with the linear least-squares fit to the data.

Mechanism of the structural transition

From these kinetic and equilibrium analyses, a schematic mechanism of the structural transition of $d(G_4T_4G_4)$ induced by Ca^{2+} is presented as shown in Figure 5. In this mechanism, once at least two Ca^{2+} ions bind to the antiparallel G-quadruplex, the structural transition from the antiparallel to the parallel G-quadruplex is induced. On the other hand, if Ca^{2+} stabilizes an unfolded state of the antiparallel G-quadruplex, which leads to the structural transition and formation of the G-wire, k_{obs} decreases with the increasing of $[d(G_4T_4G_4)]$. However, k_{obs} does not depend on $[d(G_4T_4G_4)]$ as shown in Figure 3B. Therefore, the effect of Ca^{2+} on the structure of $d(G_4T_4G_4)]$ is not stabilization of the unfolded state of the antiparallel G-quadruplex but destabilization of the antiparallel G-quadruplex structure. Thus, this k_{obs} dependency on $[d(G_4T_4G_4)]$ also supports the sequential mechanism shown in Figure 5.

Wyatt *et al*. proposed a mechanism for the formation of a parallel-stranded tetrameric G-quadruplex from single strands in which four single strands are in fast pre-equilibrium with two dimers and then the two dimers form the parallel G-quadruplex (36). Hardin *et al*. also presented a mechanism for the formation of a parallel-stranded G-quadruplex, which includes assembly intermediates (37). Their results show that an intermediate state including the dimers exists in the parallel G-quadruplex formation. Although the observation and mechanism of the structural transition from the antiparallel to the parallel G-quadruplex induced by Ca^{2+} revealed here is new, these mechanisms of parallel G-quadruplex formation from single strands support our mechanism of the structural transition in which an intermediate state exists. The parallel-stranded structure induced by Ca^{2+} may be unstable, and therefore spontaneously forms a G-wire structure, as shown on the right side of Figure 5. Previously, two structures of G-wire were proposed. One possible G-wire structure is that parallel strands position alternately via G-quartets as model 1 in Figure 5 (38,39). Another structure is that the parallel strands are linked with the thymine loops positioned on the out side of the G-quartets, and G-quadruplex can form G-wire with the stacking interactions between G-quartets as model 2 in Figure 5 (17). It should be noted that the SEC profile of $d(G_4T_4G_4)$ in the presence of Ca^{2+} was very broad (Fig. 2), indicating the existence of molecules of varying molecular masses. These SEC measurements also suggest that the structures of $d(G_4T_4G_4)$ in the presence of Ca^{2+} include not only a homogeneous four-stranded parallel G-quadruplex but also higher-ordered structures such as the G-wire. The results shown in Figure 1A and that of the CD spectra of the parallel G-quadruplex and G-wire are very similar (40), also suggest that a higher-order structure (G-wire) can only form under the conditions in which all strands are oriented in the parallel

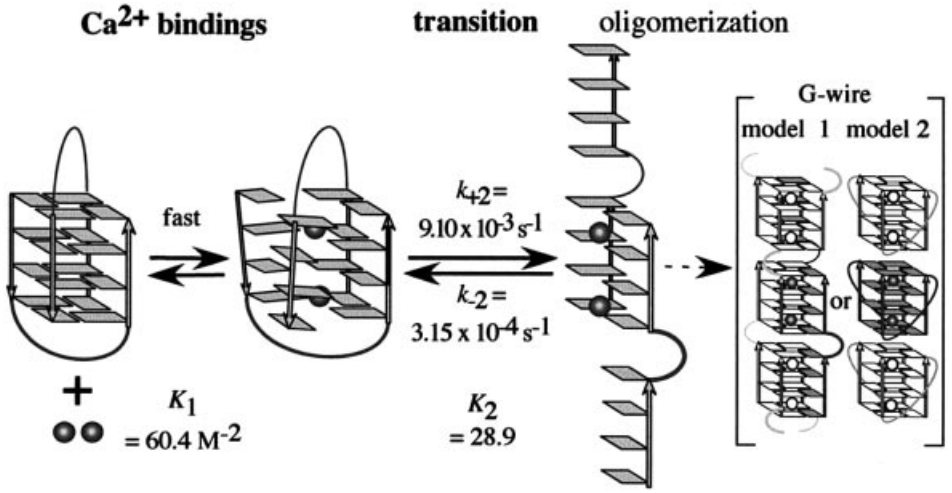

Figure 5. Schematic mechanism of the structural transition of $d(G_4T_4G_4)$ from antiparallel to parallel G-quadruplex induced by Ca^{2+}. Arrows indicate the strand directions. The guanine bases of $d(G_4T_4G_4)$ are shown as rectangles. Thymine bases in the loop have been omitted for clarity. Disks indicate Ca^{2+}.

direction. The kinetic mechanism of the structural transition and G-wire formation reported here may elucidate a general model of parallel G-quadruplex and G-wire formation, in which there is an intermediate state as shown in Figure 5.

The G-wire formation of $d(G_4T_4G_4)$ in the absence and presence of Ca^{2+} was also confirmed by AFM (Fig. S1). In the absence of Ca^{2+}, there is no particular image, indicating that $d(G_4T_4G_4)$ does not form a higher-order structure, whereas a higher-order structure was observed in the presence of Ca^{2+}. Henderson and co-workers reported the AFM images of $d(G_4T_2G_4)$ in the presence of Mg^{2+} (39). They showed that the G-wire of $d(G_4T_2G_4)$ is a linear polymer, and the height and width of the G-wires of $d(G_4T_2G_4)$ was uniform with a few bends or kinks. The length of the G-wires $d(G_4T_2G_4)$ ranged from 10 to >1000 nm. The AFM image obtained here indicates that the height and length of the images ranged from 2 to 3 nm and 10 to 400 nm, respectively. These dimensions of the AFM image of $d(G_4T_4G_4)$ are similar to the G-wire of $d(G_4T_2G_4)$. Although the AFM image obtained here is not so clear compared with that of $d(G_4T_2G_4)$, it is possible to conclude that the parallel G-quadruplex structure of $d(G_4T_4G_4)$ in the presence of Ca^{2+} finally forms the G-wire structure. Since the G-wire structure is a higher-order structure formed by the well controlled and regulated alignment of numerous DNA strands with the G-quartets as illustrated in Figure 5, the G-wire is useful for developing biomolecular materials and in biomolecular nano-engineering.

Binding site of Ca^{2+} for $d(G_4T_4G_4)$

Previously, we reported that 1 mM divalent cations destabilize the antiparallel G-quadruplex of $d(G_4T_4G_4)$ (13), corresponding to the binding step as shown in Figure 5. Ca^{2+} can coordinate with and be positioned at the center of the four guanine planes (G-quartet) and/or at a central location between the two G-quartets when the antiparallel structure of $d(G_4T_4G_4)$ is destabilized and its O6 sites are accessible. The binding constant of Ca^{2+} ions for $d(G_4T_4G_4)$ estimated from the data of the kinetics is 60.4 M^{-2} (Table 1). Interestingly, the small binding constants of cations for the G-quadruplexes were also reported previously. Hud *et al.* investigated the competition between Na^+ and K^+ for coordination by the G-quartet of $d(G_3T_4G_3)$ using NMR, and showed that the equilibrium constants for the displacement of two Na^+ by two K^+ from $d(G_3T_4G_3)$ is 13.5–21.5 (24). They suggested that a cation hydration is important to determine the ion selectivity of a G-quadruplex. Miura and Thomas reported a phase diagram of the antiparallel and parallel G-quadruplex regulated by $[Na^+]$ and $[K^+]$ using FT-Raman spectroscopy (41). The midpoints of the $[Na^+]$ and $[K^+]$ required for the structural transition are 225 and 65 mM, respectively. These reports together with our results presented here indicate that a cation binding constant for a G-quadruplex is small due to dehydration of the cation, because full dehydration of the cation must be required to coordinate the O6.

We investigated the structural transition of 25 μM $d(G_4T_4G_4)$ induced by 100 mM Ca^{2+} in the presence of various concentrations of Na^+ at 45°C to reveal that the effect of Ca^{2+} on the transition is synergetic or competitive with Na^+. The k_{obs} decreases with the increasing Na^+ concentration (data not shown), indicating the competition between Ca^{2+} and Na^+ for coordination by the G-quadruplex of $d(G_4T_4G_4)$. This competition demonstrates that the essential binding site of Ca^{2+} and Na^+ for formation of the parallel G-quadruplex is the same. In addition, the CD spectra of 25 μM $d(G_4T_4G_4)$ in a buffer containing 100 mM $CaCl_2$ and 50 mM MES (pH 6.1) shows the typical CD spectra of a parallel G-quadruplex, indicating that the parallel G-quadruplex formation does not require Na^+, and Ca^{2+} coordinates to the guanine O6 because it is essential to form the G-quartet. Thus, all the results lead to the conclusion that at least one of the coordination sites of Ca^{2+} for $d(G_4T_4G_4)$, which is essential for the antiparallel to parallel structural transition, is the guanine O6.

CONCLUSIONS

In this study, we reported the thermodynamic and kinetic analyses of the structural transition from the antiparallel to

parallel G-quadruplex and the direct observation of the G-wire formation of $d(G_4T_4G_4)$ induced by Ca^{2+}. The kinetic data showed that once Ca^{2+} ions bind to the antiparallel G-quadruplex, then the structural transition from the antiparallel to the parallel G-quadruplex and the G-wire formation are induced. The thermodynamic and kinetic data indicate that at least two Ca^{2+} ions induce the structural transition by coordination to guanine O6. Because the cation coordination to guanine O6 is crucial for the structure and stability of a G-quadruplex, many investigations of the relationship between the G-quadruplex structures and cations have focused on ionic radius. We have shown in the present study that Ca^{2+} induces a drastic structural transition of the antiparallel quadruplex, although the ionic radius of Ca^{2+} (0.99 Å) is almost the same as that of Na^+ (0.97 Å). These results show that not only the ionic radius but also other properties of cations including the energy of dehydration and/or coordination number must be considered in order to elucidate the general rules of the effect of cations on quadruplex structures.

There are few kinetic reports of the G-quadruplex structure, especially G-wire formation, although kinetic data are essential to investigate the structural transition and formation. The kinetic data revealed here showed the multi-step mechanism of the structural transition. The structural transition includes at least three steps, Ca^{2+} bindings, isomerization and oligomerization. The activation enthalpy and activation entropy were positive, suggesting the existence of disordered and/or partly broken structure that is required for the isomerization from the *syn* to *anti* glycosyl torsion angle of the guanine bases in the structural transition. Finally, the kinetic analysis indicates that the oligomerization spontaneously occurs to form the G-wire as shown in SEC and AFM measurements. This is the first report of the detailed analyses of the structural transition and G-wire formation combining kinetics and equilibrium data. The quantitative data is useful to construct a nanomaterial using the structural polymorphism of the G-quadruplex.

We found that not only the intermolecular antiparallel G-quadruplex of $d(G_4T_4G_4)$ but also the intermolecular antiparallel $d(G_3T_3G_3)$ and intramolecular antiparallel $d[(G_4T_4)_3G_4]$ undergo the structural transition induced by Ca^{2+} (Fig. 1). This suggests that the structural transition induced by Ca^{2+} is one of the general features of the antiparallel-stranded G-quadruplex. The present mechanism of the structural transition and the G-wire formation also supported by previous reports of parallel G-quadruplex formations from single strands. Therefore, the mechanism suggests a general one for the parallel G-quadruplex and G-wire formation of guanine-rich oligonucleotides. In addition, we recently reported that molecular crowding with a neutral polymer such as poly(ethylene glycol) induced the antiparallel to parallel structural transition of $d(G_4T_4G_4)$, while molecular crowding with a polycation such as putrescine did not alter the structure of the antiparallel G-quadruplex (42). Combining these results with the present study, the structural polymorphism of G-quadruplex can be generated and regulated by surrounding conditions such as monovalent and divalent cations and molecular crowding. These results suggest that the surrounding conditions of biomacromolecules should be considered in the investigation of biomacromolecular structure, stability and function.

SUPPLEMENTARY MATERIAL

Supplementary Material is available at NAR Online.

ACKNOWLEDGEMENT

This work was supported in part by Grants-in-Aid from the Ministry of Education, Science, Sports and Culture, Japan, to N.S.

REFERENCES

1. Williamson,J.R., Raghuraman,M.K. and Cech,T.R. (1989) Monovalent cation-induced structure of telomeric DNA: the G-quartet model. *Cell*, **59**, 871–880.
2. Basu,S., Szewczak,A.A., Cocco,M. and Strobel,S.A. (2000) Direct detection of monovalent metal ion binding to a DNA G-quartet by 205Tl NMR. *J. Am. Chem. Soc.*, **122**, 3240–3245.
3. Keniry,M.A. (2001) Quadruplex structures in nucleic acids. *Biopolymers*, **56**, 123–146.
4. Bock,L.C., Griffin,L.C., Latham,J.A., Vermaas,E.H. and Toole,J.J. (1992) Selection of single-stranded DNA molecules that bind and inhibit human thrombin. *Nature*, **355**, 564–566.
5. Williamson,J.R. (1994) G-quartet structures in telomeric DNA. *Annu. Rev. Biophys. Biomol. Struct. Biol.*, **23**, 703–730.
6. Kettani,A., Kumar,R.A. and Patel,D.J. (1995) Solution structure of a DNA quadruplex containing the fragile X syndrome triplet repeat. *J. Mol. Biol.*, **254**, 638–656.
7. Blackburn,E.H. (1994) Telomeres: no end in sight. *Cell*, **77**, 621–623.
8. Arthanari,H. and Bolton,P.H. (2001) Functional and dysfunctional roles of quadruplex DNA in cells. *Chem. Biol.*, **72**, 1–10.
9. Macaya,R.F., Schultze,P., Smith,F.W., Roe,J.A. and Feigon,J. (1993) Thrombin-binding DNA aptamer forms a unimolecular quadruplex structure in solution. *Proc. Natl Acad. Sci. USA*, **90**, 3745–3749.
10. Jing,N. and Hogan,M.E. (1998) Structure-activity of tetrad-forming oligonucleotides as a potent anti-HIV therapeutic drug. *J. Biol. Chem.*, **273**, 34992–34999.
11. Forman,S.L., Fettinger,J.C., Pieraccini,S., Gottarelli,G. and Davis,J.T. (2000) Toward artificial ion channels: a lipophilic G-quadruplex *J. Am. Chem. Soc.*, **122**, 4060–4067.
12. Sugimoto,N., Toda,T. and Ohmichi,T. (1998) Reaction field for efficient porphyrin metallation catalysis produced by self-assembly of a short DNA oligonucleotide. *Chem. Commun.*, 1533–1534.
13. Miyoshi,D., Nakao,A., Toda,T. and Sugimoto,N. (2001) Effect of divalent cations on antiparallel G-quartet structure of $d(G_4T_4G_4)$. *FEBS Lett.*, **496**, 128–133.
14. Chen,F.M. (1997) Supramolecular self-assembly of $d(TGG)_4$, synergistic effects of K^+ and Mg^{2+}. *Biophys. J.*, **73**, 348–356.
15. Chen,F.M. (1992) Sr^{2+} facilitates intermolecular G-quadruplex formation of telomeric sequences. *Biochemistry*, **31**, 3769–3776.
16. Venczel,E.A. and Sen,D. (1993) Parallel and antiparallel G-DNA structures from a complex telomeric sequence. *Biochemistry*, **32**, 6220–6228.
17. Parkinson,G.N., Lee,M.,P. and Neidle,S. (2002) Crystal structure of parallel quadruplexes from human telomeric DNA. *Nature*, **417**, 876–880.
18. Sugimoto,N., Nakano,M. and Nakano,S. (2000) Thermodynamics-structure relationship of single mismatches in RNA–DNA duplexes. *Biochemistry*, **39**, 11270–11281.
19. Ohmichi,T., Nakano,S., Miyoshi,D. and Sugimoto,N. (2002) Long RNA dangling end has large energetic contribution to duplex stability. *J. Am. Chem. Soc.*, **124**, 10367–10372.
20. Richard,E.G. (1975) *Handbook of Biochemistry and Molecular Biology: Nucleic Acids*, 3rd Edn. CRC Press, Cleveland, UK, Vol. 1, p. 597.
21. Balagurumoorthy,P., Brahmachari,S.K., Mohanty,D., Bansal,M. and Sasisekharan,V. (1992) Hairpin and parallel quartet structures for telomeric sequences. *Nucleic Acids Res.*, **20**, 4061–4067.
22. Jin,R., Gaffney,B.L., Wang,C., Jones,R.A. and Breslauer,K.J. (1992) Thermodynamics and structure of a DNA tetraplex: a spectroscopic and calorimetric study of the tetramolecular complexes of $d(TG_3T)$ and $d(TG_3T_2G_3T)$. *Proc. Natl Acad. Sci. USA*, **89**, 8832–8836.

23. Schultze,P., Smith,F.W. and Feigon,J. (1994) Refined solution structure of the dimeric quadruplex formed from the Oxytricha telomeric oligonucleotide d(GGGGTTTTGGGG). *Structure*, **2**, 221–233.
24. Hud,N.V., Smith,F.W., Anet,F.A.L. and Feigon,J. (1996) The selectivity for K^+ versus Na^+ in DNA quadruplexes is dominated by relative free energies of hydration: a thermodynamic analysis by 1H NMR. *Biochemistry*, **35**, 15383–15390.
25. Hud,N.V., Schultze,P., Sklenar,V. and Feigon,J. (1999) Binding sites and dynamics of ammonium ions in a telomere repeat DNA quadruplex. *J. Mol. Biol.*, **285**, 233–243.
26. Sclavi,B., Sullivan,M., Chance,M.R., Brenowitz,M. and Woodson,S. (1998) RNA folding at millisecond intervals by synchrotron hydroxyl radical footprinting. *Science*, **279**, 1940–1943.
27. Russell,R., Millett,I.S., Doniach,S. and Herschlag,D. (2000) Small angle X-ray scattering reveals a compact intermediate in RNA folding. *Nature Struct. Biol.*, **7**, 367–370.
28. Sugimoto,N., Kierzek,R. and Turner,D.H. (1988) Kinetics for reaction of a circularized intervening sequence with CU, UCU, CUCU and CUCUCU: mechanistic implications from the dependence on temperature and on oligomer and Mg^{2+} concentrations. *Biochemistry*, **27**, 6384–6392.
29. Sugimoto,N., Tomka,M., Kierzek,R., Bevilacqua,P.C. and Turner,D.H. (1989) Effects of substrate structure on the kinetics of circle opening reactions of the self-splicing intervening sequence from *Tetrahymena thermophila*: evidence for substrate and Mg^{2+} binding interactions. *Nucleic Acids Res.*, **17**, 355–371.
30. Russell,R. and Herschlag,D. (1999) New pathways in folding of the Tetrahymena group I RNA enzyme. *J. Mol. Biol.*, **291**, 1155–1167.
31. Li,Y., Bevilacqua,P.C., Mathews,D. and Turner,D.H. (1995) Thermodynamic and activation parameters for binding of a pyrene-labeled substrate by the Tetrahymena ribozyme: docking is not diffusion-controlled and is driven by a favorable entropy change. *Biochemistry*, **34**, 14394–14399.
32. Walter,N.G., Hampel,K.J., Brown,K.M. and Burke,J.M. (1998) Tertiary structure formation in the hairpin ribozyme monitored by fluorescence resonance energy transfer. *EMBO J.*, **17**, 2378–2391.
33. Fang,X.W., Pan,T. and Sosnick,T.R. (1999) Mg^{2+}-dependent folding of a large ribozyme without kinetic traps. *Nature Struct. Biol.*, **6**, 1091–1095.
34. Emerick,V.L., Pan,J. and Woodson,S.A. (1996) Analysis of rate-determining conformational changes during self-splicing of the Tetrahymena intron. *Biochemistry*, **35**, 13469–13477.
35. Bhuyan,A.K. and Udgaonkar,J.B. (1999) Observation of multistate kinetics during the slow folding and unfolding of barstar. *Biochemistry*, **38**, 9158–9168.
36. Wyatt,J.R., Davis,P.W. and Freier,S.M. (1996) Kinetics of G-quartet-mediated tetramer formation. *Biochemistry*, **35**, 8002–8008.
37. Hardin,C.C., Perry,A.G. and White,K. (2001) Thermodynamic and kinetic characterization of the dissociation and assembly of quadruplex nucleic acids. *Biopolymers*, **56**, 147–194.
38. March,T.C. and Henderson,E. (1994) G-wires: self-assembly of a telomeric oligonucleotide, d(GGGGTTGGGG), into large superstructures. *Biochemistry*, **33**, 10718–10724.
39. Marsh,T.C., Vesenka,J. and Henderson,E. (1995) A new DNA nanostructure, the G-wire, imaged by scanning probe microscopy. *Nucleic Acids Res.*, **23**, 696–700.
40. Protozanova,E. and Macgregor,R.B.,Jr (1998) Circular dichroism of DNA frayed wires. *Biophys. J.*, **75**, 982–989.
41. Miura,T., Benevides,J.M. and Thomas,G.J.,Jr (1995) A phase diagram for sodium and potassium ion control of polymorphism in telomeric DNA. *J. Mol. Biol.*, **248**, 233–238.
42. Miyoshi,D., Nakao,A. and Sugimoto,N. (2002) Molecular crowding regulates the structural switch of the DNA G-quadruplex. *Biochemistry*, **42**, 15017–15024.